

# Digital Operating Mode Classification of Real-World Amateur Radio Transmissions

Maximilian Bundscherer, Thomas H. Schmitt, Ilja Baumann and Tobias Bocklet

*Technische Hochschule Nürnberg Georg Simon Ohm*

Nuremberg, Germany

{firstname.lastname}@th-nuernberg.de

**Abstract**—This study presents an ML approach for classifying digital radio operating modes evaluated on real-world transmissions. We generated 98 different parameterized radio signals from 17 digital operating modes, transmitted each of them on the 70 cm (UHF) amateur radio band, and recorded our transmissions with two different architectures of SDR receivers. Three lightweight ML models were trained exclusively on spectrograms of limited non-transmitted signals with random characters as payloads. This training involved an online data augmentation pipeline to simulate various radio channel impairments. Our best model, EfficientNetB0, achieved an accuracy of 93.80% across the 17 operating modes and 85.47% across all 98 parameterized radio signals, evaluated on our real-world transmissions with Wikipedia articles as payloads. Furthermore, we analyzed the impact of varying signal durations & the number of FFT bins on classification, assessed the effectiveness of our simulated channel impairments, and tested our models across multiple simulated SNRs.

**Index Terms**—Automatic Modulation Classification, Amateur Radio, Spectrum Monitoring, Cognitive Radio, Machine Learning

## I. INTRODUCTION

The ability to quickly and accurately identify primary users and other participants is essential, especially for Cognitive Radio (CR) applications where several participants use a radio band autonomously. Precise and quick classification enables CR participants to efficiently use their radio band without interfering with the transmissions of others. In addition, an automatic radio signal classification system is also essential for monitoring compliance with the frequency plan. Due to the large number of different types of radio signals, manual classifications are not economical. We utilized signal processing and Machine Learning (ML) methods to classify digital operating modes and their parameters in amateur radio scenarios exclusively on spectrograms with computer vision models. Such models can support spectrum monitoring authorities or organizations identifying band intruders, like the Federal Communications Commission (FCC).

This work is related to Automatic Modulation Classification (AMC) studies, interested in classifying the modulations of radio transmissions, e.g., Frequency-Shift Keying (FSK), Phase-Shift Keying (PSK), Multiple Frequency-Shift Keying (MFSK) or Orthogonal Frequency-Division Multiplexing (OFDM). There is another perspective of digital modulation in amateur radio, usually due to hardware limitations, which originated through the requirements of speech transmissions:

The already modulated signal in the Audio Frequency (AF) is typically transmitted via the Upper Side Band (USB) of a transceiver. In this case, the Radio Frequency (RF) is not generated directly, for example, by a specialized digital transceiver. This technique allows transmitting a similar modulated signal in the RF up to a bandwidth of 3 kHz. In amateur radio, these modulations are seen as operating modes with specific modulation parameters and specified (e.g., error-correction & synchronization) procedures, such as BPSK31 or Olivia 4/250. In this example, BPSK (a PSK modulation) and Olivia (a MFSK modulation) could be differentiated as the pure operating mode and 31 and 4/250 as parameters for these modes. This study refers to them as operating mode (OM) and operating mode parameters (OMP). The main contributions of this study are:

- Generation of 98 different parameterized radio signals from 17 digital operating modes & transmission on the 70 cm (UHF) amateur radio band. Recording these transmissions with two different architectures of SDR receivers for real-world evaluation.
- Training of the computer vision models ResNet-18, EfficientNetB0, and Vision Mamba Tiny exclusively on spectrograms of limited non-transmitted data, utilizing an online data augmentation pipeline to simulate radio channel impairments.
- Analysing the impact of varying signal durations and number of FFT bins on classification utilizing real-world radio signals.
- Evaluation of the models across multiple simulated SNRs and assessment of the simulated channel impairments.

## II. RELATED WORK

Current AMC/ML studies utilized deep learning models such as CNN/LSTM-based models [1] [2], and Transformer-based models [3] [4]. Some of them focus on feature engineering [5] [6], or data augmentation [7], and compare ML & traditional methods [8]. Multi-tasking approaches have been studied in [9]. A multi-modal approach for 5G has been presented in [10]. ML approaches not requiring labeled data for training were examined in [11] and [12]. Traditional methods can also be used for AMC, seen as feature extractors, such as Fast Fourier Transform (FFT)-based measurements [13] or wavelet-transform-based baud rate estimations [14]. ML methods are also used in digital radio communication, e.g.,

TABLE I

OVERVIEW OF OUR GENERATED SIGNALS: 98 DIFFERENT OPERATING MODE PARAMETERS (OMP) OUT OF 17 OPERATING MODES (OM).

OM	OMP
BPSK	31, 63, 63F, 125, 250, 500, 1000
QPSK	31, 63, 125, 250, 500
8PSK	125, 125F, 125FL, 250, 250F, 250FL, 500, 500F, 1000, 1000F, 1200F
MC-PSK	125C12, 250C6, 500C2, 500C4, 800C2, 1000C2
PSKR	125, 250, 500, 1000
Olivia	4/125, 4/250, 8/250, 8/500, 16/500, 16/1000, 32/1000, 64/2000
Contestia	4/125, 4/250, 4/500, 8/250, 8/500, 16/500, 32/1000, 64/2000
MFSK	4, 8, 11, 16, 22, 31, 64, 64L, 128, 128L
DominoEx	EX Micro, EX4, EX5, EX8, X11, X16, X22, X44, X88
Thor	Micro, 100, 11, 16, 22, 25x4, 4, 5, 50x1, 50x2, 8
Throb	BX1, BX2, BX4, OB1, OB2, OB4
MT63	500S, 500L, 1000S, 1000L, 2000S, 2000L
OFDM	500F, 750F, 3500
RTTY	RTTY
IFKP	IFKP
CW	CW
Noise	Noise

deep-learning-based channel estimation [4]. The challenge of classifying a signal can be extended with simultaneous detection [15]. The studies [16] [17] also deal with detecting and classifying one or more signals in wideband scenarios. Most of these studies utilized synthetic data, e.g., the RADIOML 2016.10A dataset [18], or generated synthetic data for evaluation [3]. An exception is [19], in which the signals were transmitted within a room, and [20], which classified real-world ADS-B signals. This study utilized methods from the fields of telecommunications, Digital Signal Processing (DSP), Software-Defined Radio (SDR), and amateur radio. A comprehensive overview of wireless communication can be found in [21]. In [22] and [21], the impairments that affect radio channels in real environments, such as path loss, fading, and interference, are described in detail. We used DSP algorithms for filtering and processing the recordings of our transmissions, which can be read about in [23]. These are also described more in detail in the context of SDR receivers in [24] and [25]. An overview of digital modulation techniques can be found in [26]. A detailed explanation of the digital amateur radio modes can be found in [27].

### III. DATA

#### A. Radio Signal Generation & Overview

We generated radio signals of digital modes used in (amateur) radio communication. These modes include traditional methods, such as CW/Morse; and FSK modes, such as RTTY; more modern modes, like PSK modes, such as BPSK31; and modes with significantly higher bandwidths, such as MFSK and OFDM modes. Each of these modes is characterized by mode-related parameters that determine, for example, the signal bandwidth, the baud rate, and the size of the modulation alphabet. As shown in Table I, we generated 98 different parameterized radio signals (OMP) from 17 digital operating modes (OM) by utilizing Fldigi [28], which radio amateurs

and emergency services widely use for digital communication. We generated 180s for training  $D_{Train}$  and 60s for validation  $D_{Val}$  for each OMP with random characters as payloads in AF.

#### B. Radio Signal Transmission, Recording & Postprocessing

We used distinct Wikipedia article excerpts as payloads for  $D_{Test}$  and generated 75s for each OMP for our USB-transmission with a Kenwood TS-2000X with about 5 Watt. We recorded these transmissions using an RTL-SDR, a heterodyne receiver, and a HackRF, a direct-conversion receiver. The RTL-SDR is referred to as R0, and the HackRF as R1. Both SDR receivers were operated with a sampling rate of 1 MHz with a frequency offset of 200 kHz related to the transmission frequency, providing complex I/Q baseband representations. Ground Plane Antennas were used for both the transmitter and the receivers. R0 and R1 were located in different locations to reduce the risk of local interference, and the transmitter was about 1 km away from both. Due to the urban environment, both receivers had no line of sight with the transmitter.

From the recorded complex I/Q baseband data, a narrow-band channel centered at the transmission frequency was extracted for R0 and R1. Each channel was filtered to a bandwidth of 3 kHz (6 kHz sampling rate). The complex I/Q signals were then USB demodulated to obtain real-valued representations. A channel bandwidth of 3 kHz was selected to ensure direct compatibility with standard amateur radio equipment. Therefore, the computation of the spectrograms for the classification can be performed directly on the AF output of a transceiver (e.g., via the jack connection) or a WebSDR receiver (via a virtual microphone). Based on our data generation specifications, we automatically cut and labeled all 98 OMP per receiver. These data sets are referred to as  $D_{Test/R0}$  and  $D_{Test/R1}$ . We achieved an Signal-to-Noise Ratio (SNR) of approx. 35 dB with R0 and 31 dB with R1. After 4h of transmission, a maximum frequency drift of 14 Hz was measured at R0 and 160 Hz at R1.

## IV. METHODS

#### A. Classification Models

This study focuses on two CNN-based models: ResNet-18 (RN-18) (11.4M params) [29], EfficientNetB0 (EN-B0) (5.3M params) [30], and a Vision Transformer: Vision Mamba Tiny (Vim-Ti) (7M params) [31]. RN-18 was selected due to its proven effectiveness as a classic CNN model. EN-B0 was selected because it can achieve a higher classification accuracy with fewer parameters on ImageNet [32]. Vim-Ti was included as it represents a state-of-the-art Vision Transformer model. We selected the tiniest model from each family. All models were pre-trained on ImageNet [32], as preliminary experiments have shown that using non pre-trained models reduced accuracy by an average of 26%. We considered the spectrograms of our signals as images and used them for all three input channels of our models. We trained our models with Cross-Entropy loss. We applied Early Stopping with a patience of 5 to limit the potential risk of overfitting. As a

training algorithm, we applied Stochastic Gradient Descent (SGD) with a learning rate of 0.001 and a momentum of 0.9. The batch size was set to 256. We chose SGD over Adam as the optimizer, as it showed more stable behavior during our training across all models.

### B. Online Data Augmentation & Channel Impairments

We showed in preliminary experiments with all of our models that training on the limited data set  $D_{Train}$  is not practical if the models are evaluated on real-world transmitted data  $D_{Test/R0}$  and  $D_{Test/R1}$ . One reason is that we only have 180s of data per OMP in AF, and real-world radio transmissions are affected by various radio channel impairments [21] [22]. We, therefore, utilized an online data augmentation pipeline for the simulation of channel impairments and the expansion of our data for training, including the following augmentations:

*Amplify*: Scales the amplitude of the recording by a specified factor. *FreqShift*: Shifts the recording frequency by a specified amount in Hz. It applies a complex exponential to the waveform, effectively shifting its frequency components. The shifted signal is filtered to remove the lower sideband, and the result is converted back to a real-valued representation. *SimTone*: Adds a simulated single-tone interference to the recording. It generates a sine wave at a specified frequency and amplitude. This tone is added to the recording. *Noise*: Adds Gaussian White Noise to the recording to match a specified SNR in dB. For  $D_{Train}$  and  $D_{Val}$ , these augmentations were applied in the following order:

$$Aug = \{Amplify, FreqShift, SimTone_1, SimTone_2, Noise\}$$

For  $D_{Train}$ , this sequence was applied five times, with an additional instance of unaugmented data:

$$D'_{Train} = \{Aug(D_{Train})_1, \dots, Aug(D_{Train})_5, D_{Train}\}$$

The augmentation parameters were randomly selected each time an augmentation was applied within these ranges: Amplify  $\in [0.1, 2]$ , FreqShift  $\in [-500, 500]$ , SimTone<sub>1/2</sub>  $\in ([10, 2990]; [0, 0.3])$ , and Noise  $\in [-6, 42]$ . For  $D'_{Val}$  the same augmentation sequence was applied once without unaugmented data and with fixed parameters: Amplify 0.5, FreqShift 400, SimTone<sub>1</sub> 1000;0.03, SimTone<sub>2</sub> 2300;0.015 and Noise 30.

In this way, we provided new unseen training data with random channel impairments at each training epoch. During training, we validated our models on a fixed set that mimics a concrete real-world scenario. No augmentation was applied on our real-world test datasets  $D_{Test/R0}$  and  $D_{Test/R1}$ .

## V. EXPERIMENTS & RESULTS

Our preliminary experiments showed that training on signals in AF is impractical for models evaluated on real-world transmissions influenced by various radio channel impairments; see Table II. We conducted a channel impairment study to assess the impact of our simulated impairments on real-world classification. In this study, we successively excluded all augmentations to evaluate their impact on real-world classification

TABLE II

THE ACCURACIES WITH AND WITHOUT DATA AUGMENTATIONS OF OUR OPERATING MODE PARAMETERS (OMP) (98 CLASSES) AND OPERATING MODE (OM) (17 CLASSES) CLASSIFICATIONS WITH EFFICIENTNET-B0 (EN-B0), CONSIDERING A DURATION OF 2S AND 128 FFT BINS.

EVALUATED ON OUR REAL-WORLD TRANSMISSIONS, RECORDED BY A HETERODYNE (R0) AND A DIRECT-CONVERSION (R1) SDR RECEIVER. IN THE SECOND PART OF THE TABLE, A SPECIFIC DATA AUGMENTATION IN TRAINING WAS REMOVED TO ASSESS ITS IMPACT ON CLASSIFICATION.

Augmentation	R0		R1	
	OMP [%]	OM [%]	OMP [%]	OM [%]
without all Augs.	3.14	8.23	3.03	7.35
with all Augs.	84.05	92.64	79.74	89.88
-Amplify	78.90	87.59	58.14	64.70
-FreqShift	83.35	92.05	42.45	57.74
-SimTone <sub>1</sub>	83.90	92.61	81.19	90.02
-SimTone <sub>1/2</sub>	80.67	90.57	74.41	84.75
-Noise	4.73	11.90	5.23	17.21

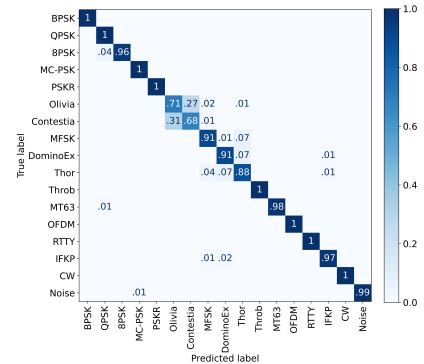


Fig. 1. This normalized confusion matrix visualizes the operating mode (OM) confusions of our best model, EfficientNet-B0 (EN-B0), considering a duration of 2s and 128 FFT bins. Evaluated for both receivers R0 and R1.

accuracies. As noted in Table II, e.g., our *Noise* augmentation proved particularly important for training our models. This study also investigated the impact of varying signal durations and the number of FFT bins on classification evaluated on our real-world datasets. To explore this, we conducted experiments with our three models with separate training and evaluation for each combination across the signal durations of 1s, 2s, 3s, 4s, and 64, 128, 256 FFT bins for spectrogram computation. The results of these experiments are detailed in Table III.

EN-B0 performed the best of our models with an accuracy of 93.80% across the 17 OM and 85.47% across all 98 OMP. The accuracy significantly increased when the signal was analyzed for at least 2s for classification. We aimed to minimize the signal duration while maintaining meaningful classification, enabling higher robustness through multiple decisions in real-world scenarios. Therefore, we selected our best model, EN-B0, for further evaluation in this study, considering a duration of 2s. Figure 1 shows that most confusion occurred between Contestia and Olivia. Finally, we evaluated our best model EN-B0 across multiple simulated SNRs. Figure 2 presents the classification accuracy of EN-B0 with 128 FFT bins across  $-6$  and  $27$  dB with varying durations.

We trained our models intending to classify OMP and evaluate our models with the datasets  $D_{Test/R0}$  and  $D_{Test/R1}$

TABLE III  
THE ACCURACIES OF OUR OPERATING MODE PARAMETERS (OMP) (98 CLASSES) AND OPERATING MODE (OM) (17 CLASSES) CLASSIFICATIONS. EVALUATED ON OUR REAL-WORLD TRANSMISSIONS, RECORDED BY A HETERODYNE (R0) AND A DIRECT-CONVERSION (R1) SDR RECEIVER.

Dur	n-FFT	EfficientNetB0 (EN-B0)		ResNet-18 (RN-18)		Vision Mamba Tiny (Vim-Ti)	
		OMP [%]	OM [%]	OMP [%]	OM [%]	OMP [%]	OM [%]
4s	256	<b>85.47 ± 0.94</b>	<b>93.80 ± 0.75</b>	81.58 ± 3.69	90.48 ± 2.85	<b>84.40 ± 2.27</b>	<b>92.91 ± 2.01</b>
4s	128	84.89 ± 0.87	93.46 ± 0.52	<b>84.21 ± 2.38</b>	92.51 ± 1.79	80.83 ± 4.31	89.94 ± 3.48
4s	64	81.02 ± 4.33	89.51 ± 4.11	82.99 ± 4.67	<b>93.12 ± 1.80</b>	81.08 ± 4.18	90.20 ± 3.41
3s	256	<b>83.81 ± 1.31</b>	92.20 ± 1.43	79.24 ± 4.13	88.91 ± 3.51	<b>82.93 ± 2.04</b>	92.40 ± 1.30
3s	128	83.73 ± 1.34	<b>92.60 ± 0.98</b>	81.81 ± 2.15	90.25 ± 2.19	80.92 ± 4.03	89.34 ± 3.76
3s	64	82.35 ± 3.02	90.46 ± 3.20	<b>82.10 ± 3.86</b>	<b>91.80 ± 2.55</b>	82.64 ± 2.95	<b>92.42 ± 1.43</b>
2s	256	81.67 ± 2.01	90.39 ± 1.98	77.40 ± 4.65	87.02 ± 4.42	81.22 ± 1.86	90.72 ± 1.72
2s	128	<b>81.90 ± 2.16</b>	<b>91.26 ± 1.38</b>	<b>81.06 ± 2.27</b>	89.92 ± 2.01	78.28 ± 4.53	88.57 ± 3.67
2s	64	81.17 ± 2.86	90.51 ± 2.39	79.78 ± 5.15	<b>90.21 ± 2.57</b>	<b>81.94 ± 1.89</b>	<b>90.72 ± 1.72</b>
1s	256	77.48 ± 2.44	87.23 ± 2.34	73.12 ± 3.73	83.82 ± 3.75	<b>76.89 ± 3.06</b>	86.89 ± 2.59
1s	128	77.62 ± 3.05	<b>87.81 ± 2.32</b>	<b>76.30 ± 1.55</b>	<b>86.61 ± 1.84</b>	76.62 ± 4.17	86.70 ± 3.71
1s	64	<b>77.63 ± 3.94</b>	87.16 ± 3.14	74.33 ± 4.67	85.92 ± 2.64	77.75 ± 2.45	<b>87.93 ± 1.94</b>

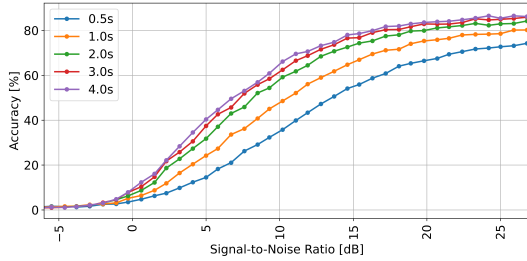


Fig. 2. The operating mode parameters (OMP) classification accuracies of our best model, EfficientNet-B0 (EN-B0), utilizing 128 FFT bins across multiple simulated SNRs.

from the receivers R0 and R1 with both the classification task OMP and OM. To ensure comparability, we trained separate models for each possible combination of varying durations and the number of FFT bins. To ensure comparability across models trained with varying durations, we extracted the same amount of classification windows from  $D_{Test/R0}$  and  $D_{Test/R1}$  using a consistent shift of 0.5s, maintaining an equal number of evaluation decisions for all configurations. In our case, 75s per OMP, which means up to 150 decisions are made per OMP and receiver for evaluation. With 98 different OMP, this means 14.700 decisions per receiver.

## VI. DISCUSSION

It can be noted that *Noise* augmentation was the most important of all our augmentations; see Table II. The *FreqShift* augmentation was particularly important for R1, as this receiver was also affected by a higher frequency drift; see Section III-B. The receivers were also influenced by unavoidable radio interference, which is why the (multiple) application of *SimTone* can be helpful for this scenario. This local interference also constantly influences the gain control of SDR receivers, and the real-world signals are typically received with different SNR, which is where *Amplify* can support. As shown in Table III, EN-B0 performed the best of our models. It can be noted that the duration of a signal was more important than the choice of the number of FFT bins for classification. The accuracy significantly increased when the

signal was analyzed for at least 2s for classification. Most of the confusion occurred within an OM and between Contestia and Olivia; see Figure 1. Contestia is a modification of Olivia that has been specially adapted for higher speeds and more robust transmissions under the conditions of amateur radio competitions. For example, the encoding has been optimized for transmission speed by only allowing the transmission of capital letters. The transmitted signal, therefore, does not differ in most parts. The OMs MFSK, DominoEx, and Thor are similarly close to each other. Figure 2 shows that a longer signal resulted in a more meaningful classification even at a poorer SNR. Above approx. 25 dB SNR, the accuracy no longer changed significantly for the better. The methods employed and the design decisions, such as selecting a channel width of 3 kHz, ensure that our approach is lightweight & compatible with standard amateur radio equipment and WebSDR receivers for direct integration; see Sections III-B and IV-A.

## VII. CONCLUSION

With limited non-transmitted data (180s) per OMP in AF with random characters as payloads, it was possible to train our three ML models exclusively on spectrograms successfully. By evaluating our models on real-world transmissions, we showed that adding artificial noise across multiple SNR conditions and applying a frequency shift augmentation was necessary for successful training. Our best model, EfficientNetB0, achieved an accuracy of 93.80% across the 17 OM and 85.47% across all 98 OMP. In general, it can also be noted that longer signal durations significantly enhanced classification accuracy, especially under challenging SNR conditions. In future studies, we will analyze the differences in classification at real-world poor SNR compared to the simulated ones.

## ACKNOWLEDGMENT

We would like to thank the TH Nürnberg for using their amateur radio station DF0OHM and Prof. Dr. Thomas Lauterbach for his advice on radio topics. This study was supported by the Bavarian Collaborative Research Program (Bayerischen Verbundforschungsprogramms, BayVFP) under grant ID DIK0517/02.

## REFERENCES

- [1] A. Emam, M. Shalaby, M. A. Aboelazm, H. E. Abou Bakr, and H. A. Mansour, "A comparative study between cnn, lstm, and cldnn models in the context of radio modulation classification," in *2020 12th International Conference on Electrical Engineering (ICEENG)*. IEEE, 2020, pp. 190–195.
- [2] T. Huynh-The, C.-H. Hua, Q.-V. Pham, and D.-S. Kim, "Mcnet: An efficient cnn architecture for robust automatic modulation classification," *IEEE Communications Letters*, vol. 24, no. 4, pp. 811–815, 2020.
- [3] L. Boegner, M. Gulati, G. Vanhoy, P. Vallance, B. Comar, S. Kokalj-Filipovic, C. Lennon, and R. D. Miller, "Large scale radio frequency signal classification," *arXiv preprint arXiv:2207.09918*, 2022.
- [4] Z. Chen, F. Gu, and R. Jiang, "Channel estimation method based on transformer in high dynamic environment," in *2020 International Conference on Wireless Communications and Signal Processing (WCSP)*, 2020, pp. 817–822.
- [5] X. Zhao, X. Zhou, J. Xiong, F. Li, and L. Wang, "Automatic modulation recognition based on multi-dimensional feature extraction," in *2020 International Conference on Wireless Communications and Signal Processing (WCSP)*. IEEE, 2020, pp. 823–828.
- [6] F. Meng, P. Chen, L. Wu, and X. Wang, "Automatic modulation classification: A deep learning enabled approach," *IEEE Transactions on Vehicular Technology*, vol. 67, no. 11, pp. 10760–10772, 2018.
- [7] L. Huang, W. Pan, Y. Zhang, L. Qian, N. Gao, and Y. Wu, "Data augmentation for deep learning-based radio modulation classification," *IEEE access*, vol. 8, pp. 1498–1506, 2019.
- [8] S. Peng, H. Jiang, H. Wang, H. Alwageed, and Y.-D. Yao, "Modulation classification using convolutional neural network based deep learning model," in *2017 26th Wireless and Optical Communication Conference (WOCC)*. IEEE, 2017, pp. 1–5.
- [9] S. Chang, S. Huang, R. Zhang, Z. Feng, and L. Liu, "Multitask-learning-based deep neural network for automatic modulation classification," *IEEE internet of things journal*, vol. 9, no. 3, pp. 2192–2206, 2021.
- [10] P. Qi, X. Zhou, S. Zheng, and Z. Li, "Automatic modulation classification based on deep residual networks with multimodal information," *IEEE Transactions on Cognitive Communications and Networking*, vol. 7, no. 1, pp. 21–33, 2020.
- [11] K. Davaslioglu, S. Boztaş, M. C. Ertem, Y. E. Sagduyu, and E. Ayanoglu, "Self-supervised rf signal representation learning for nextg signal classification with deep learning," *IEEE Wireless Communications Letters*, vol. 12, no. 1, pp. 65–69, 2022.
- [12] Z. Chen, H. Cui, J. Xiang, K. Qiu, L. Huang, S. Zheng, S. Chen, Q. Xuan, and X. Yang, "Signet: A novel deep learning framework for radio signal classification," *IEEE Transactions on Cognitive Communications and Networking*, vol. 8, no. 2, pp. 529–541, 2021.
- [13] S. Scholl, "Exact signal measurements using fft analysis," 2016.
- [14] Y. Gao, Y. Wan, L. Li, and J. Men, "Baud rate estimation of fsk signals based on wavelet transform," in *2012 Second International Conference on Intelligent System Design and Engineering Application*. IEEE, 2012, pp. 181–184.
- [15] A. Vagollari, V. Schram, W. Wicke, M. Hirschbeck, and W. Gerstacker, "Joint detection and classification of rf signals using deep learning," in *2021 IEEE 93rd Vehicular Technology Conference (VTC2021-Spring)*. IEEE, 2021, pp. 1–7.
- [16] L. Boegner, G. Vanhoy, P. Vallance, M. Gulati, D. Feitzinger, B. Comar, and R. D. Miller, "Large scale radio frequency wideband signal detection & recognition," *arXiv preprint arXiv:2211.10335*, 2022.
- [17] B. Comar, "Modulation recognition using yolov5 on the wbsig53 dataset," in *2023 32nd Wireless and Optical Communications Conference (WOCC)*. IEEE, 2023, pp. 1–6.
- [18] T. J. O'shea and N. West, "Radio machine learning dataset generation with gnu radio," in *Proceedings of the GNU radio conference*, vol. 1, no. 1, 2016.
- [19] T. J. O'Shea, T. Roy, and T. C. Clancy, "Over-the-air deep learning based radio signal classification," *IEEE Journal of Selected Topics in Signal Processing*, vol. 12, no. 1, pp. 168–179, 2018.
- [20] T. Ya, L. Yun, Z. Haoran, J. Zhang, W. Yu, G. Guan, and M. Shiwen, "Large-scale real-world radio signal recognition with deep learning," *Chinese Journal of Aeronautics*, vol. 35, no. 9, pp. 35–48, 2022.
- [21] T. S. Rappaport, *Wireless Communications - Principles and Practice*. New Jersey: Prentice Hall PTR, 2002.
- [22] D. Tse and P. Viswanath, *Fundamentals of Wireless Communication*. Cambridge: Cambridge University Press, 2005.
- [23] R. G. Lyons, *Understanding Digital Signal Processing*. Amsterdam: Pearson Education, 2010.
- [24] A. Heuberger and E. Gamm, *Software Defined Radio-Systeme für die Telemetrie - Aufbau und Funktionsweise von der Antenne bis zum Bit-Ausgang*. Berlin Heidelberg New York: Springer-Verlag, 2017.
- [25] J. H. Reed, *Software Radio - A Modern Approach to Radio Engineering*. New Jersey: Prentice Hall Professional, 2002.
- [26] J. G. Proakis, *Digital Communications*. New York: McGraw-Hill, 2008.
- [27] S. Ford, *ARRL's HF Digital Handbook*. American Radio Relay League, 2007.
- [28] D. Freese, "Fldigi," <http://www.w1hkj.com/>, 2023.
- [29] K. He, X. Zhang, S. Ren, and J. Sun, "Deep residual learning for image recognition," in *Proceedings of the IEEE conference on computer vision and pattern recognition*, 2016, pp. 770–778.
- [30] M. Tan and Q. Le, "EfficientNet: Rethinking model scaling for convolutional neural networks," in *Proceedings of the 36th International Conference on Machine Learning*, ser. Proceedings of Machine Learning Research, K. Chaudhuri and R. Salakhutdinov, Eds., vol. 97. PMLR, 09–15 Jun 2019, pp. 6105–6114. [Online]. Available: <https://proceedings.mlr.press/v97/tan19a.html>
- [31] L. Zhu, B. Liao, Q. Zhang, X. Wang, W. Liu, and X. Wang, "Vision mamba: Efficient visual representation learning with bidirectional state space model," *arXiv preprint arXiv:2401.09417*, 2024.
- [32] J. Deng, W. Dong, R. Socher, L.-J. Li, K. Li, and L. Fei-Fei, "Imagenet: A large-scale hierarchical image database," in *2009 IEEE conference on computer vision and pattern recognition*. Ieee, 2009, pp. 248–255.